1980ApJ...238..808R

THE ASTROPHYSICAL JOURNAL, 238:808–817, 1980 June 15
© 1980. The American Astronomical Society. All rights reserved. Printed in U.S.A.

VELOCITIES AND MASS DISTRIBUTION IN THE BARRED SPIRAL NGC 5728

VERA C. RUBIN[1]
Department of Terrestrial Magnetism, Carnegie Institution of Washington
Received 1979 September 4; accepted 1979 December 12

ABSTRACT

NGC 5728 is classified as a barred spiral galaxy, although its morphology is of the lens or oval disk type. Velocities near the nucleus indicate rotational motions, but with large ($V \sim 250$ km s^{-1}) outward streaming motions. Beyond the center, the disk rotates with apparent constant *angular* velocity to the edge of the disk, $r = 16$ kpc, where the oval disk merges with two very faint open arms. The mass in the disk plus bulge is 10^{11} $\mathfrak{M}_\odot$, with 80% coming from the constant density disk. The velocity structure is generally in agreement with velocities predicted by theoretical models of barred spiral galaxies which incorporate a small nonaxisymmetric perturbing potential.

Subject headings: galaxies: individual — galaxies: internal motions — galaxies: structure

I. INTRODUCTION AND OBSERVATIONS

Our current study of extended rotation curves of spiral galaxies has been restricted almost entirely to nonbarred galaxies. One exception is NGC 5728, a previously unstudied southern galaxy ($\alpha_{1950} = 14^h39^m.6$; $\delta = -17°2'.4$), classified SAB(r)a (de Vaucouleurs, de Vaucouleurs, and Corwin 1976). Although no distinct bar is detected on our plate material, NGC 5728 is a member of that class of lens or oval disk galaxies called barred by Sandage. On the basis of a blue plate taken with the Las Campanas 2.5 m duPont telescope (Fig. 1 [Pl. 23]), it is classified SBb(s)II (Sandage and Brucato 1979). de Vaucouleurs generally calls such oval disk galaxies SAB types. Surrounding the nucleus, an amorphous lens-shaped region is interrupted by a prominent dust lane, originating West of the nucleus and extending to the NE. The corresponding dust lane to the SW is less distinct. A string of bright knots marks the regions where the lens or oval disk joins the outer spiral structure. Two very faint open outer arms emerge at the ends of the lens, too faint to show in Figure 1. NGC 5728 bears a remarkable resemblance to NGC 613 (Burbidge *et al.* 1964) and NGC 1097 (Sandage 1961), although the outer arms are less well developed in NGC 5728. NGC 5728 has no nearby companion.

It is not clear whether in NGC 5728 we are observing an ovally distorted disk or a lens (Kormendy 1979; see also Kormendy and Norman 1979), i.e., a distinct elliptical structure intermediate between a spheroid and a disk. NGC 5728 is most likely a transition case between early-type galaxies which contain clearly differentiated lenses and late types in which oval disks are common. Although I shall generally refer to the NGC 5728 structure as a lens, this classification is tentative and based partly on the dynamics discussed below. The central structure of NGC 5728 is curiously asymmetric (Fig. 1). A high luminosity nucleus (diameter ~4″), centrally located with respect to the lens, sits asymmetrically within a nuclear ring (dimensions 7″.5 × 10″). The nucleus is tangent to the ring on the E; the W edge of the ring extends almost to the absorption lane. The ring appears to be a real structure, and not an effect due to obscuration. A weak Hα plate taken by Ford with the 1.8 m Perkins telescope of the Ohio State and Ohio Wesleyan Universities at Lowell Observatory at a high spatial scale shows only the 4″ nucleus and the star to the NE; the ring is not a strong emitter of Hα. Although rings may be a common feature in nuclei of barred spirals (NGC 1097: Sersic and Pastoriza 1965; NGC 3351: Rubin, Ford, and Peterson 1975), no asymmetry like that in NGC 5728 has previously been noted. With the distance of 54 Mpc adopted below, the nucleus, ring, and lens have radii of 0.5 kpc, 1.0 × 1.3 kpc, and 20 kpc, respectively.

Spectra of NGC 5728 have been obtained with the CTIO 4 m spectrograph plus Carnegie (C33063) image tube, at dispersions of 50 and 25 Å mm^{-1}; a record of observations is given in Table 1, and the Hα regions of all spectra are reproduced in Figure 2 (Plate 24). In the nucleus ($r \sim 2''$) strong lines of Hα, [N II] λλ6548, 6583, and [S II] λλ6717, 6731 are observed, with [N II] marginally stronger than Hα and the [S II] lines of equal intensity. Weaker lines of [O I] λλ6300, 6364 and [Ar III] λ7136 are also present. The presence of [Ar III] implies moderate excitation; the He I lines generally seen in spectra of high excitation (He I λλ5876, 6678, and 7065) are not observed. The Na I D lines present in absorption are relatively narrow and resolved (separation 6 Å). The velocity dispersion for the stars in the nucleus is low, lower, for example, than in M31 (σ_v

[1] Visiting Astronomer, Cerro Tololo Inter-American Observatory, which is supported by the National Science Foundation under contract AST 74-0412B.

© American Astronomical Society • Provided by the NASA Astrophysics Data System

1980ApJ...238..808R

TABLE 1

SPECTROSCOPIC OBSERVATIONS OF NGC 5728

Plate	Date (1978 Feb)	Dispersion (Å mm^{-1})	P.A. (degrees)	Exposure (min)	Extent of Emission
1031	5	50	33	153[a]	58″NE–60″SW
1035	10	50	90	45	7″E–8″W
1039	11	50	123	25	6″SE–11″SW
1045a	24	25	33	29	55″NE–58″SW
1045b	24	25	63	28	4″NE–7″SW
1046a	24	25	93	27	4″SE–5″NW
1046b	24	25	123	24	7″SE–7″NW

[a] All plates N_2 baked IIIa-J.

= 190 km s^{-1}; Schecter and Gunn 1979) where the Na I D lines are completely blended (Rubin, Ford, and Kumar 1973). This observation suggests that the stars in the nucleus do not share the complex velocities which are seen in the gas. Just off the nucleus and also at large r the emission is weaker overall and Hα is stronger than [N II].

In the nuclear spectra, the Hα and [N II] emission lines are split into multiple components, arising from a complex velocity pattern. The emission continues beyond the nucleus through the region of the nuclear ring. Nuclear emission is intense; emission from the ring is weak (Fig. 2). To the SW, the separation of the ring from the nucleus seen on the direct plate (Fig. 1*b*) is seen also in the spectra.

II. THE VELOCITY FIELD OF NGC 5728

The curious nuclear velocity patterns shown in Figure 2 complicate the velocity measurements; an attempt has been made to measure velocities of all the principle knots. Generally, the velocity of the center of gravity of a knot is measured, but in the cases denoted by brackets in Table 2 extreme velocities are also obtained. The measured heliocentric velocities are tabulated in Table 2, and plotted in Figures 3 and 5. Velocities are generally accurate to 10 or 15 km s^{-1} per point.

For the disk of NGC 5728 I measure the following parameters: major-axis position angle, $\phi = 33°$; minor axis to major axis ratio, $(b/a) = 0.58$; neglecting the very faint unmeasurable outer arms. The velocities indicate that the NE major axis is approaching, so the NW side is the near side if the spiral arms are trailing. This conclusion is consistent with the pattern of absorption seen on the NW.

Along the major axis, P.A. = 33°, velocities are near 175 km s^{-1} with respect to the nucleus, $0'' < r < 10''$ (< 1 kpc). At larger distances $25'' < r < 60''$ ($6.5 < r < 16$ kpc), velocities are symmetrical about $V_0 = 2800$ km s^{-1} and increase linearly with r (Fig. 3). In the range $10 < r < 16$ kpc, the increase is such that V/R is almost (but not quite) constant. This can be demonstrated by placing a straight edge through the measured velocities passing through $V_0 =$

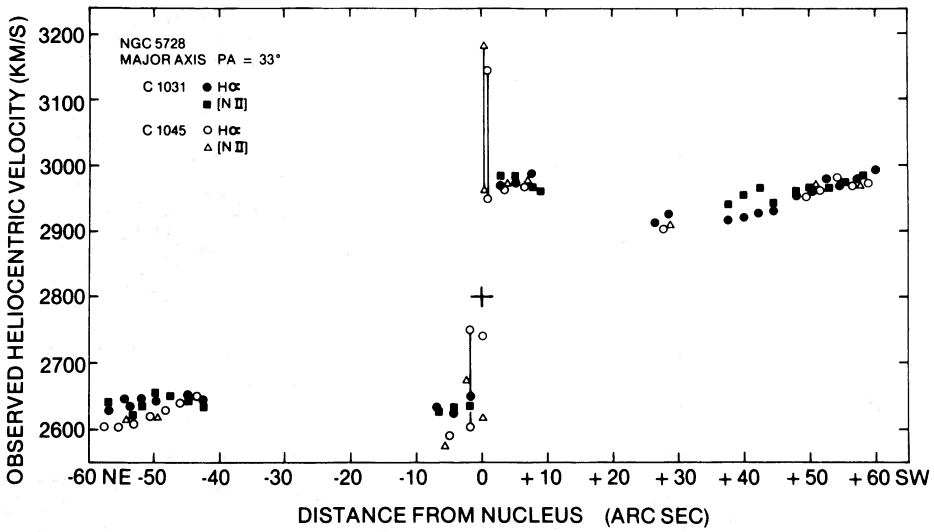

FIG. 3.—Observed heliocentric velocities as a function of distance from the nucleus for NGC 5728 from two plates. Velocities measured from broad lines are shown connected by lines. At large r, velocities rise almost linearly with r; this can be shown by placing a ruler through plotted points and origin (+), $V = 2800$ km s^{-1}.

© American Astronomical Society • Provided by the NASA Astrophysics Data System

1980ApJ...238..808R

TABLE 2

MEASURED HELIOCENTRIC VELOCITIES IN NGC 5728

Plate / Line	S (arcsec)	V (km s^{-1})
C1031 PA 33°		
Hα	NE −56.7	2630
	−54.3	2645
	−53.4	2638
	−52.0	2644
	−49.6	2646
	−44.9	2651
	−42.5	2646
	−6.5	2630
	−4.1	2626
	−1.7	2650
	+3.1	2969
	+5.4	2977
	+7.7	2988
	+26.6	2912
	+28.9	2925
	+37.8	2917
	+40.2	2920
	+42.5	2928
	+44.8	2931
	+48.2	2955
	+50.6	2961
	+52.9	2977
	+55.3	2970
	+57.6	2980
	SW +60.0	2992
[NII]	−56.7	2643
	−54.3	2643
	−53.3	2622
	−52.0	2644
	−49.6	2652
	−47.3	2650
	−44.9	2648
	−42.5	2639
	−6.5	2631
	−4.0	2627
	−1.8	2634
	+3.1	2985
	+5.4	2980
	+7.7	2968
	+9.0	2962
	+37.8	2940
	+40.1	2956
	+42.5	2965
	+44.8	2943
	+48.2	2958
	+50.6	2967
	+53.0	2965
	+55.3	2969
	+57.7	2983
C1045b PA 63°		
Hα	NE −3.7	2745
	−0.4	3029
	−0.1	[2874
		[3196
	+3.9	2872
	SW +6.9	2893
[NII]	−4.5	2673
	−3.0	2777
	−0.1	2979
	−0.1	[2833
		[3184
	+3.4	2904
	+6.2	2912
C1045a PA 33°		
Hα	NE −57.6	2605
	−55.3	2605
	−53.0	2610
	−50.6	2621
	−48.3	2630
	−46.0	2640
	−43.6	2650
	−5.0	2595
	−1.9	[2602
		[2748
	+0.2	2740
	+0.8	[2948
		[3142
	+3.5	2965
	+6.8	2969
	+27.8	2902
	+49.6	2951
	+51.9	2963
	+54.2	2981
	+56.6	2969
	SW +59.0	2973
[NII]	−54.0	2619
	−50.0	2622
	−5.6	2579
	−2.3	2675
	+0.3	2617
	+0.7	[2965
		[3184
	+3.6	2964
	+7.4	2974
	+28.2	2904
	+50.4	2969
	+57.4	2969
C1035 PA 90°		
Hα	E −5.0	2755
	−2.4	2775
	+0.8	3147
	+3.5	2487
	+4.2	2774
	W +7.4	2807
[NII]	−7.3	2751
	−5.0	2776
	−2.6	2786
	+4.1	2652
	+4.4	2763
	+8.0	2817
C1046a PA 93°		
Hα	SE −3.2	2755
	−3.2	[2695
		[2822
	+0.4	3002
	+0.4	[2893
		[3149
	+1.6	2537
	+4.5	2716
	+4.6	2771
	NW +4.7	2831
[NII]	−3.7	2768
	−3.0	[2720
		[2853
	+0.3	3005
	+0.3	[2887
		[3162
	+1.7	2572
	+4.1	[2720
		[2831
	+4.5	2777
C1046b PA 123°		
Hα	SE −6.9	2796
	−4.2	2829
	−4.2	[2740
		[2912
	−0.3	3033
	−0.3	[2909
		[3162
	+0.5	2552
	+0.5	[2450
		[2646
	+2.7	2679
	NW +5.6	2689
[NII]	−7.4	2806
	−4.6	2854
	−4.6	[2753
		[2911
	−0.7	3022
	−0.7	[2891
		[3158
	+0.5	2585
	+0.5	[2460
		[2672
	+3.9	2675
	+6.6	2725
C1039 PA 123°		
Hα	SE −6.3	2796
	−3.8	2837
	−1.0	2910
	−0.8	3269
	+0.7	3210
	+1.9	2616
	+2.2	3103
	+3.8	2694
	+5.9	2770
	+8.0	2808
	NW +10.7	2715
[NII]	−6.4	2831
	−4.4	2868
	−1.9	2925
	−1.4	3223
	+0.6	3282
	+1.6	2623
	+2.1	3102
	+3.3	2683
	+5.2	2769
	+7.5	2809
	+10.6	2656

Hα: λ6562.817
[NII]: λ6583.400

© American Astronomical Society • Provided by the NASA Astrophysics Data System

1980ApJ...238..808R

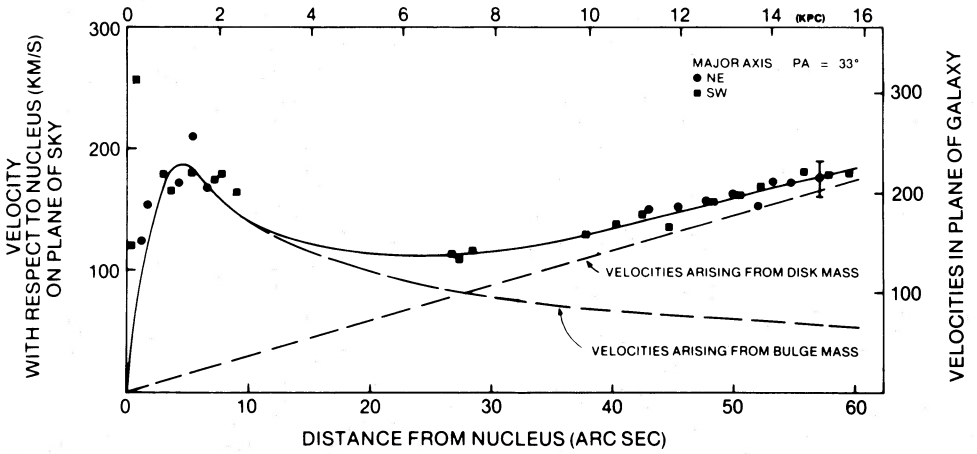

FIG. 4.—Adopted rotation curve for NGC 5728 (*solid line*) superposed upon measured velocities. The mass distribution is resolved into two components, one a centrally condensed bulge producing velocities V_B which decrease approximately as $r^{-1/2}$ (*long-dashed line*) and one a constant density disk producing velocities $V_D \propto r$ (*short-dashed line*). The rotation curve is given by $V = (V_B^2 + V_D^2)^{1/2}$.

2800 km s^{-1}. Thus, if we assume that beyond the central region the measured velocities represent circular velocities, the outer galaxy is rotating with almost solid-body rotation. Such a velocity pattern at nuclear distances as great as 16 kpc is never observed for spiral galaxies without bars.

The mean velocities at each r (formed from the measured velocity of Hα and [N II] on the two major-axis plates), when reflected through $V_0 = 2800$ km s^{-1}, produce the velocity curve shown in Figure 4. The velocity scatter near the nucleus appears real, and may indicate very rapid rotation at very small r. Beyond the nucleus, the NE and SW velocities agree well. If only circular velocities were present, the smooth curves in Figure 4 would be the rotation curve for NGC 5728. However, both the observed central velocities and the theory (discussed below) imply noncircular motions. We defer until § III a discussion of the mass distribution inferred from the observed velocities, and the dependence of this derived mass on the geometry and the noncircular motions. For the systemic velocity we adopt $V_0 = 2800$ km s^{-1}; $V_c = 2710$ km s^{-1} corrected for a solar velocity of 300 km s^{-1} with respect to the Local Group. With $H = 50$ km s^{-1} Mpc^{-1}, the distance of NGC 5728 is 54 Mpc; $1'' = 262$ pc.

We now discuss the velocities in the central region. If there were no perturbations arising from the presence of the oval distortion, then only circular velocities would be present, and the minor-axis velocities would be constant at the systemic velocity. Instead, in P.A. = 123° (Fig. 5), we observe a velocity $V \sim -250$ km s^{-1} at $r \sim 0$ increasing to $V \sim 0$ at $r \sim 8''$ (2 kpc) on the near minor axis, and a velocity of $V \sim$

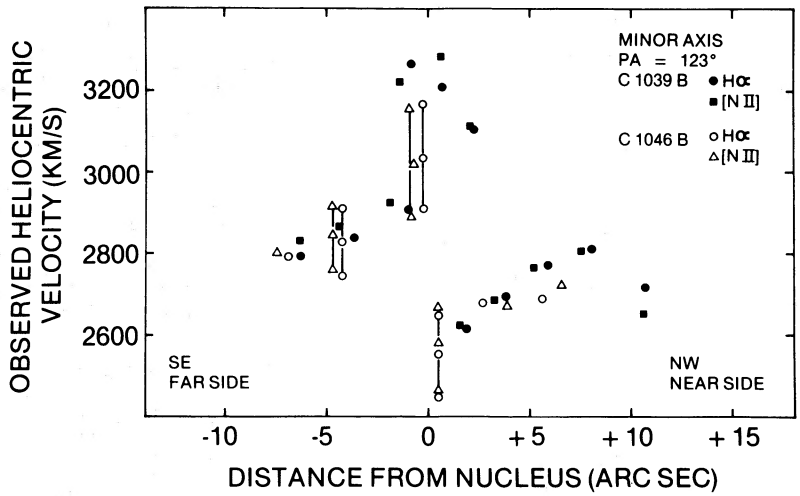

FIG. 5.—Velocities as a function of nuclear distance along minor axis, P.A. = 123°. Note that velocities are not equal to systemic velocity $V = 2800$ km s^{-1} at $r = 0$, but approach it at $r = 8''$. Also note that velocities are double valued $0'' < r < 2''$ NW; velocities from far side of ring are observed through the ring.

© American Astronomical Society • Provided by the NASA Astrophysics Data System

1980ApJ...238..808R

$+250$ km s^{-1} at $r \sim 0$ decreasing to $V \sim 0$ at $r \sim 7$ kpc (1.8 kpc) on the far side (Fig. 5). Observations of departures from circular motions in the nuclear regions of barred spirals are now commonplace (NGC 3351: Rubin, Ford, and Peterson 1975; NGC 5383: Peterson *et al.* 1978; NGC 7723: Chevalier and Furenlid 1978; NGC 1097: Wolstoncroft and Schempp 1979). Significant noncircular motions are predicted by theoretical models of barred spirals (Roberts 1979; Roberts, Huntley, and van Albada 1979; Sanders and Tubbs 1979; Huntley 1979) which show that the presence of a small (5–10%) nonaxisymmetric perturbing potential will distort the velocity field near the nucleus. We show in Figure 6 a schematic drawing of the oval, steady-state gas circulation in a Toomre disk on which has been superposed an inhomogeneous spheroidal component in the inner parts. The amplitude of the perturbing axisymmetric potential is 5.7% here. The figure, reproduced from Roberts, Huntley, and van Albada (1979), applies to galaxies such as NGC 5728, in which an inner Lindblad resonance is present. For this model, sharply pointed oval stremlines and noncircular motions with $V \sim 150$ km s^{-1} characterize the strong gas response to the shock which has formed toward the leading edge of the bar. In the inner disk, gas is directed outward along the shock; in the outer regions, gas is focused inward. This shock-focusing mechanism is assumed to be responsible for the enhanced star-forming activity near the ends of the bar. In order to match the observations of NGC 5728, noncircular central motions near $V \sim 250$ km s^{-1} are required. These would arise from a perturbing axisymmetric potential of order 10–12% (W. W. Roberts, private communication).

With this scaling, Figure 6 is now a good representation of the morphology of NGC 5728. With the near side (NW) oriented to match the bottom of Figure 6, the NE dust lane emerging from the nucleus corresponds to the near-side shock dust lane; the far-side dust lane is filled in. Our velocity observations for NGC 5728 are not comprehensive enough to make a detailed dynamical model, but in their general characteristics the velocities match the predictions of the model. Clearly, velocities measured along the minor axis in Figure 6 will show large nonzero motions.

To examine the nuclear motions, we have compared the observed line-of-sight velocities in all observed position angles with the line-of-sight velocities predicted for nuclear models with (1) rotation $V(R)$ only; (2) rotation plus axisymmetric expansion, $E(R)$; and (3) rotation only in a nucleus with $\phi \neq 33°$. Note that in the theoretical models, the streamlines near the center are noncircular, and are closed. This implies large noncircular velocities, in contrast to model (1); and no net flow of matter, in contrast to model (2). However, there could be a small inward or outward material flow, not included in the model, whose velocities contribute to those observed. Note also that while our velocity mapping is extensive in the central regions, it includes only the major-axis velocities for larger R. Hence a more detailed model is not possible.

The observed line-of-sight velocity with respect to the nucleus in position angle η is given by

$$V_{oc} = V_{\text{obs-central}} = \frac{V(R)\cos(\eta - \phi)\sin i + E(R)\sin(\eta - \phi)\tan i}{[\sec^2 i - \tan^2 i \cos^2(\eta - \phi)]^{1/2}}. \quad (1)$$

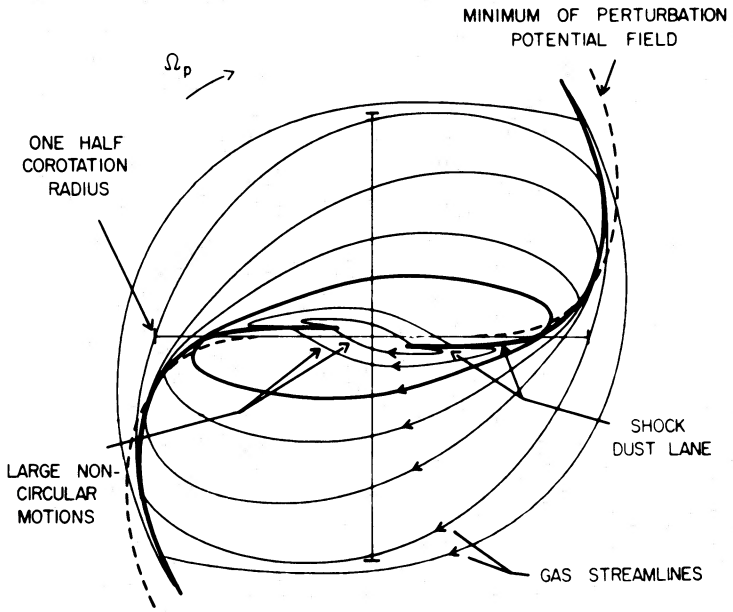

FIG. 6.—The oval, steady-state gas circulation in a galaxy composed of a thin-disk Toomre component and a small nuclear spheroidal component, from Roberts, Huntley, and van Albada (1979). Note the shock dust lane, and the skewing of the streamlines at small r, the region of large noncircular motions.

© American Astronomical Society • Provided by the NASA Astrophysics Data System

1980ApJ...238..808R

TABLE 3

NUCLEAR VELOCITIES IN NGC 5728

Velocity	Model 1 Rotation Only ($\phi = 33°$)	Model 2 Rotation Plus Expansion	Model 3 Rotation Only ($\phi \neq 33°$)
Plane of galaxy:			
$V(2\farcs5)$	304 ± 128	305	446 ± 50 ($\phi = -6°$)
$E(2\farcs5)$	0	278	0
$[\Sigma\,(\text{resid})^2]^{1/2}$	339	132	132
$V(5'')$	321 ± 66	321	386 ± 16 ($\phi = +3°$)
$E(5'')$	0	148	0
$[\Sigma\,(\text{resid})^2]^{1/2}$	175	51	42
Plane of sky[a]:			
$V(2\farcs5)$	170 ± 72	171	249 ± 28
$E(2\farcs5)$	0	155	0
$V(5'')$	180 ± 37	180	216 ± 9
$E(5'')$	0	83	0

[a] V observed along major axis; E observed along minor axis.

From the geometry of the nucleus and the ring (Fig. 1*b*) we adopt $i = 34°$ for the nuclear region.

In Figures 7*a*, 7*b*, and 7*c* we plot the observed line-of-sight velocities V_{oc} in all observed position angles, corresponding to the distance $r = 2\farcs5$ (650 pc) in the plane of the galaxy. The solid curves are least-squares fits to these observations, for rotation only (7*a*), rotation plus axisymmetric expansion (7*b*), and rotation only in a skewed disk (7*c*). Values of the rotation and expansion velocities are listed in Table 3. Figures 7*d*, 7*e*, and 7*f* plot the V_{oc} at a larger nuclear distance ($r = 5'' = 1.3$ kpc), again with least-squares fits for the three models. From Figure 7 and the calculations indicated in Table 3, we draw the following conclusions.

1. The variation of observed line-of-sight velocity with position angle near the nucleus of NGC 5728 does exhibit a sinusoid variation, as predicted by equation (1). Nuclear motions are predominantly circular. However, a simple rotating disk with the geometry

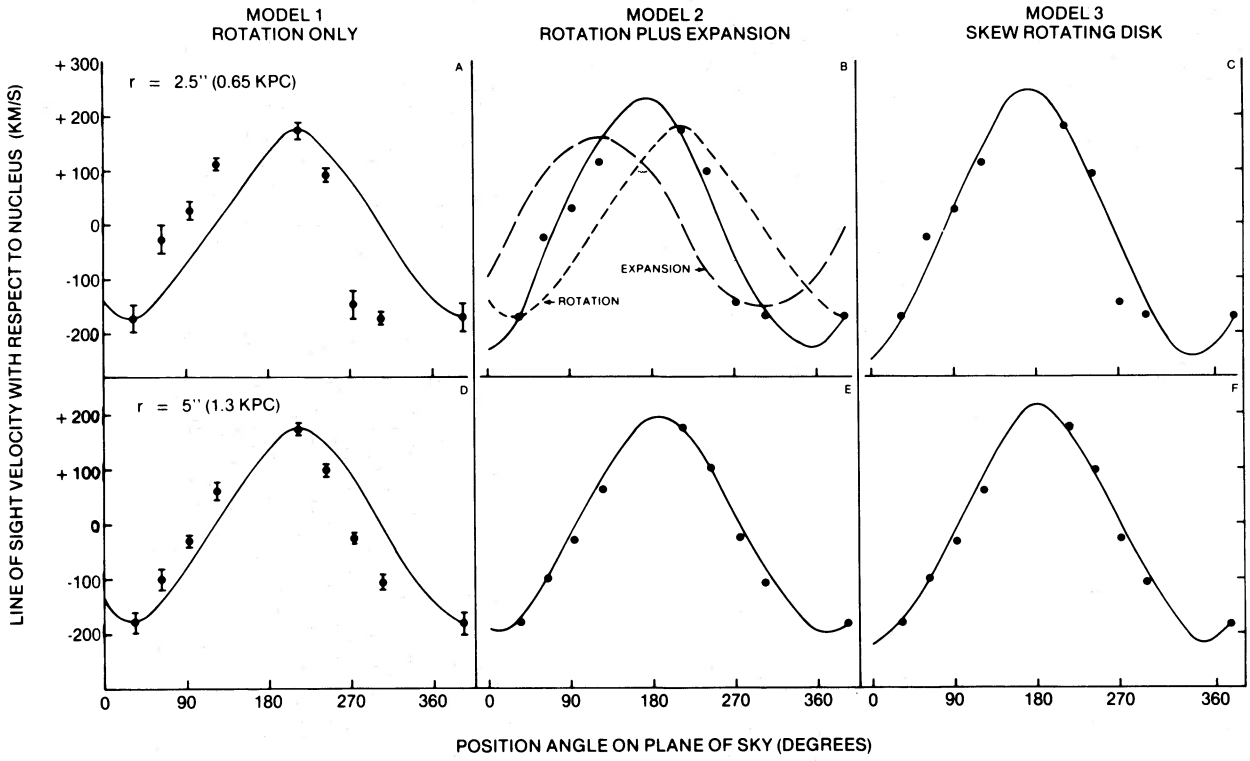

FIG. 7.—Comparison of observed velocities at $r = 2\farcs5$ and $r = 5''$, with predictions from three models. See Table 3 for details of models.

© American Astronomical Society • Provided by the NASA Astrophysics Data System

1980ApJ...238..808R

defined by the outer disk is an extremely poor fit to velocities at $r = 650$ pc, and only a slightly better fit at $r = 1.3$ kpc. As r increases, the geometry of the nucleus approaches that of the outer disk.

2. Models with rotation plus axisymmetric expansion are a much better fit to the observed velocities, and imply a constant rotational velocity near $V = 300$ km s^{-1} and an expansion velocity decreasing from $E \sim 275$ to $E \sim 150$ km s^{-1} from $r = 0.65$ to $r = 1.3$ kpc. From Figure 4 we know that $E \sim 0$ at $r \sim 2$ kpc. Simple energetic considerations show that velocities radial from the nucleus with $V \sim 250$ km s^{-1} decreasing to zero near 2 kpc imply a nuclear mass ($r \leq 2$ kpc) $\sim 1 \times 10^{10}$ $\mathfrak{M}_\odot$. This value agrees well with the mass deduced below from the rotational velocities.

3. Models with circular rotation only are an equally good fit to the velocities if they arise in a flattened disk whose apparent major axis rotates from $\phi = -6°$, $r = 0.65$ kpc to $\phi = +3°$, $r = 1.3$ kpc to $\phi = 33°$, $r \sim 2$ kpc, i.e., the angle with respect to the outer disk decreases from $\sim 40°$ at $r = 0.65$ kpc to $\sim 30°$ at $r = 1.3$ kpc to 0° at $r \sim 2$ kpc. An inner disk whose angular displacement with respect to the outer disk decreases with increasing R appears to be an adequate description of the streamlines in Figure 6. It is likely that we are actually viewing a spheroidal or triaxial nuclear bulge, so its description in terms of a circularly rotating disk is only an approximation to the real geometry.

Both models (2) and (3) are fairly good fits to the limited velocity data, and both are likely approximations to the velocities implied by the streamlines in Figure 6, with the exception of the matter flow in model (2). Both models require high velocities [$(V^2 + E^2)^{1/2} = 400$ km s^{-1}], and hence high energies, whose source we leave unspecified. There is little doubt, however, that large streaming motions near the nuclei of barred spirals are observationally well established and in general agreement with the theoretical models.

III. MASS DISTRIBUTION IN NGC 5728

The linear increase of V with r seen in the outer parts of NGC 5728 (Fig. 5) suggests the presence of a constant density disk. We have therefore used a simple mass model to deconvolve the rotation curve into two components, one arising from a nuclear mass and the other from a uniform density disk. The model is characterized by few parameters. We initially make two simplifying assumptions, (1) that the galaxy is circular in its principal plane, and (2) that only circular motions are present so the observed velocities are rotational velocities. This is equivalent to assuming that the streamlines in Figure 6 are circular.

We adopt a model with a centrally condensed bulge, of axial ratio 0.1, containing 10^{10} $\mathfrak{M}_\odot$ within 1 kpc of the center. Its radial density variation (Table 4, column [5]) is chosen so as to reproduce the velocities (column [4]), and is given approximately by $\rho_{\rm bulge} \propto R^{3.7}$. This mass produces velocities V_B which rise to $V = 226$ km s^{-1} (in the plane of the galaxy $\equiv 185$ km s^{-1} on the sky) at $r = 5''$ (1.3 kpc) and decay with $\sim r^{-1/2}$ Keplerian decrease thereafter (Fig. 4). A second mass component, a disk of uniform density $\rho = 0.05$ $\mathfrak{M}_\odot$ pc^{-3} produces velocities V_D which increase linearly from the origin with a slope 13 km s^{-1} kpc^{-1}. For comparison, the volume density in the vicinity of the Sun is 0.15 $\mathfrak{M}_\odot$ pc^{-3}. These two mass distributions combine to produce a total velocity $V = (V_B^2 + V_D^2)^{1/2}$, shown by the solid curve in Figure 4, which is a remarkably good fit to the observations.

The density variation and the integral mass of the bulge and the disk components are shown in Figure 8, as a function of distance from the nucleus, and their

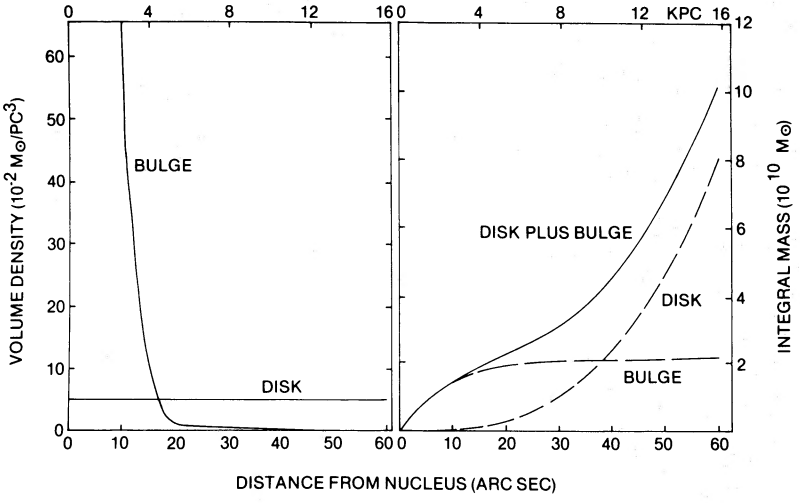

FIG. 8.—(*Left*) Volume density as a function of nuclear distance for bulge plus disk model discussed in text. (*Right*) Integral mass of disk, bulge, and disk plus bulge as a function of nuclear distance to limit of velocity observations.

© American Astronomical Society • Provided by the NASA Astrophysics Data System

1980ApJ...238..808R

TABLE 4

MASS AND DENSITY DISTRIBUTION IN NGC 5728

OBSERVED			BULGE			DISK			TOTAL	
r (arcsec) (1)	r (kpc) (2)	V (km s^{-1}) (3)	V_B (km s^{-1}) (4)	ρ (10^{-2} $\mathfrak{M}_\odot$ pc^{-3}) (5)	$\mathfrak{M}$ (10^{10} $\mathfrak{M}_\odot$) (6)	V_D (km s^{-1}) (7)	ρ (10^{-2} $\mathfrak{M}_\odot$ pc^{-3}) (8)	$\mathfrak{M}$ (10^{10} $\mathfrak{M}_\odot$) (9)	V^a (km s^{-1}) (10)	$\mathfrak{M}$ (10^{10} $\mathfrak{M}_\odot$) (11)
0	0	0	0		0	0	4.9	0	0	0
5	1.3	226	226	369	0.98	18	4.9	0.005	227	0.98
10	2.6	193	164	54	1.4	35	4.9	0.037	167	1.4
20	5.2	149	125	1.00	2.0	71	4.9	0.30	143	2.3
30	7.9	144	93	0.67	2.0	107	4.9	1.0	142	3.0
40	10.5	171	85	0.37	2.1	143	4.9	2.4	166	4.5
50	13.1	198	76	0.15	2.1	178	4.9	4.6	194	6.7
60	15.7	225	69	0.02	2.2	214	4.9	8.0	225	10.0

[a] $V_{\text{Total}} = (V_B^2 + V_D^2)^{1/2}$. All velocities in plane of galaxy; $i = 55°$.

properties are tabulated in Table 4. They have been calculated for spheroids of axis ratio $c/a = 0.1$, using the procedures developed by Burbidge, Burbidge, and Prendergast (1959). Because the derived volume density is strongly dependent upon the axial ratio of the adopted model, it is of interest to express the density also in terms of a projected surface density. At $R = 10$ kpc, the projected surface density is about 100 $\mathfrak{M}_\odot$ pc^{-2}.

To convert from velocity on the sky to velocity in the plane of the galaxy, we have here adopted $i = 55°$, which assumes that the outer contours of the disk are circular in the plane of NGC 5728. The apparent axial ratio of the disk is $b/a = 0.58$; the outer arms are too faint to measure a and b, but are probably much more circular. Hence, both the disk and the arms cannot be circular if coplanar. This circumstance is not unique, and Kormendy (1979) has demonstrated that in galaxies of lens/ring morphology, neither lens nor outer ring is circular. Axial ratios of lenses are typically 0.9 $\pm$ 0.05. If the true axial ratio of the lens is between 0.85 and 1, then the outer arms (if in the plane of the disk) have a true axial ratio far from unity. However, the error in the mass introduced by the assumption of circularity is probably less than 25%; this estimate is based on the likely range of inclinations.

The error introduced by assuming circular velocities is harder to assess, because of our limited velocity coverage beyond the center. From Figure 6 we see that the streamlines become more nearly circular with increasing R, and we know from model 3 that at $R = 5'' = 1.3$ kpc the angle between the central dynamical major axis and the outer galaxy contours is 30°. It seems likely that in the region 8–16 kpc (where the outer velocities are observed), the angle between the major axis and the streamlines will have decreased to no more than 15°. The outermost observed velocities are probably very close to circular velocities.

An upper limit to the mass can be found by assuming that there is significant mass at large R, so the "true" rotation curve is flat at $V \sim 225$ km s^{-1}, i.e., at the highest observed velocity. Then the apparent decrease of V with decreasing R (from 16 to 8 kpc) results from the increasing angle between the streamlines and the line of sight. With this approximation, the mass is of order $\mathfrak{M} \sim 1.3 \times 10^{11}$ $\mathfrak{M}_\odot$ compared with $\mathfrak{M} = 1 \times 10^{11}$ $\mathfrak{M}_\odot$ calculated assuming circular orbits. We conclude that the mass calculated on the assumption of circular orbits and a circular outer envelope is a lower limit and could be larger by a factor up to 2.

The combined bulge plus disk mass out to $r = 16$ kpc is therefore $\mathfrak{M}_{16} \sim 1.0 \times 10^{11}$ $\mathfrak{M}_\odot$, with 80% located in the disk. The integrated mass is still rising precipitously at $r = 16$ kpc; significant mass must be located beyond this distance. de Vaucouleurs, de Vaucouleurs, and Corwin (1976) give $r = 22$ kpc as the radius where the surface brightness has fallen to 25 mag arcsec^{-2}, and Griersmith (1979) gives $r = 38$ kpc, where it has fallen to 26 mag arcsec^{-2}. Thus these velocity observations cover 71% of the r_{25}; $\mathfrak{M}_{22}$ must be at least 2×10^{11} $\mathfrak{M}_\odot$.

An indication of the gross variation of integral mass to integral blue luminosity, $\mathfrak{M}/L_B$, across NGC 5728 can be found from the concentric aperture photometry of Griersmith (1979). His observations, $B = 13.87$, 13.09, and 12.56, through apertures corresponding to radii of 4, 8, and 38 kpc, produce $\mathfrak{M}/L_B$ of 1.3, 1.2, and ≥ 2 (in solar units) corrected for extinction, inclination, and redshift. Hence the ratio of mass to blue luminosity is fairly constant over the optical image, $R \leq 15.7$ kpc.

IV. DISCUSSION AND CONCLUSIONS

NGC 5728 is a barred spiral galaxy with a peculiar nucleus, a lens or an oval disk, and two open outer spiral arms. A small nucleus sits tangent on one side to a nuclear ring. Velocities in the nuclear region indicate that the isovelocity contours are skewed with respect to those for a rotating disk aligned with the outer lens. This observation of large streaming motions near the nucleus is consistent with predictions from theoretical models by W. W. Roberts, Sanders, Huntley, and collaborators, who have shown that the presence of a

© American Astronomical Society • Provided by the NASA Astrophysics Data System

1980ApJ...238..808R

small (5–10%) perturbation in the axisymmetric potential produces large streaming motions in the gas near the nucleus.

Beyond the nucleus, in the region of the lens, the gas rotates with almost constant angular velocity, out to $r = 16$ kpc, the region where the lens merges with the two open outer arms. The mass distribution of NGC 5728 can be described in terms of a $2 \times 10^{10}\ \mathfrak{M}_\odot$ bulge mass superposed upon a constant density disk of mass $8 \times 10^{10}\ \mathfrak{M}_\odot$ out to $r = 16$ kpc. These masses come from a model which assumes that the disk is circular in the plane of the galaxy, and that the streamlines are circular. While it is difficult to assess the numerical effect of these assumptions, it is likely that the error in the mass and density is less than a factor of 2.

These observations of NGC 5728 lend support to two facts based on velocity fields of very few barred spiral galaxies. First, large velocity streaming exists near the nucleus. Second, angular velocities are constant in the region of the bar or lens. Large noncircular gas motions are seen in the nucleus of NGC 3351 (Rubin, Ford, and Peterson 1975), in NGC 5385 (Peterson *et al.* 1978), in NGC 7723 (Chevalier and Furenlid 1978), in NGC 1097 (Wolstoncroft and Schempp 1979), and now in NGC 5728. Constant angular velocity is observed in the stellar motions along the bar in NGC 3351 (Peterson *et al.* 1976), and in the gas motions in NGC 7479 (Burbidge, Burbidge, and Prendergast 1960), in NGC 7723, in NGC 6764 (Rubin, Thonnard, and Ford 1975), and possibly in NGC 613 (Burbidge *et al.* 1964), although it was not recognized as such by its authors. NGC 5728 probably is barred, and thus supports this earlier conclusion. Alternatively, NGC 5728 may be showing us that lenses too rotate almost as solid bodies. In NGC 5728, the region of constant angular velocity extends to $r = 16$ kpc, a considerable fraction of the galaxy radius.

Beyond the region of the bar, the form of the rotation curve is known for only a few barred galaxies. For NGC 7723, the rotation curve is flat; for NGC 3351, velocities decrease with increasing R in the ring region. Morphologically, NGC 3351 is unlike 5728 and 1097. Observations of more barred spirals at large nuclear distances will be necessary to learn if there is a preferred form for the rotation curve beyond the bars.

Suddenly it appears that barred spirals are less of an enigma. Considerable understanding of their dynamics has come from the interplay of theoretical and observational studies of their morphology and velocities. Theoretical work, which started with Prendergast's unpublished but widely quoted suggestion that the straight dust lanes in barred spirals mark the locus of shocked gas, now extends to computer models which reproduce the major morphological and dynamical properties of barred spirals. The superposition of a small nonaxisymmetric potential due to the bar upon the normal galaxy potential is the major ingredient of such models. Other approaches in relating the dynamics to the spiral density wave model (Chevalier and Furenlid 1978; Lynden-Bell 1979) and in detailing the morphological components of barred spirals (Kormendy 1979) have also contributed to this understanding.

The most striking property of the kinematics of NGC 5728 is the approximately constant angular velocity extending completely across its lens. Given the present limited sample of velocity fields for barred spirals, it is not too much of a simplification to state that beyond their central regions barred spirals rotate with constant *angular* velocity, while nonbarred spirals rotate with constant *circular* velocity. A similar conclusion, based on theoretical considerations of rotating and collapsing spherical gas clouds, was reached significantly earlier by Mestel (1963), with even fewer rotation curves available.

I thank Dr. Victor Blanco, the Director of the Cerro Tololo Inter-American Observatory, for making telescope time available; Drs. W. K. Ford, Jr. and A. Sandage for the plates of NGC 5728; Allan Rubin for help with the calculations; Dr. D. Griersmith for supplying the magnitudes; and Dr. W. W. Roberts for supplying Figure 6 and confirming that velocity fields in barred spirals are not hopelessly confused. I also thank the referee, Dr. John Kormendy, who clarified many points concerning lenses and ovals in spiral galaxies.

REFERENCES

Burbidge, E. M., Burbidge, G. R., and Prendergast, K. H. 1959, *Ap. J.*, **130**, 26.
———. 1960, *Ap. J.*, **132**, 654.
Burbidge, E. M., Burbidge, G. R., Rubin, V. C., and Prendergast, K. H. 1964, *Ap. J.*, **140**, 80.
Chevalier, R. A., and Furenlid, I. 1978, *Ap. J.*, **225**, 67.
de Vaucouleurs, G., de Vaucouleurs, A., and Corwin, H. G. 1976, *Second Reference Catalogue of Bright Galaxies* (Austin: University of Texas Press).
Griersmith, D. 1979, Ph.D. thesis, Australian National University.
Huntley, J. M. 1979, preprint.
Kormendy, J. 1979, *Ap. J.*, **227**, 714.
Kormendy, J., and Norman, C. 1979, *Ap. J.*, **233**, 539.
Lynden-Bell, D. 1979, *M.N.R.A.S.*, **187**, 101.
Mestel, L. 1963, *M.N.R.A.S.*, **126**, 553.
Peterson, C. J., Rubin, V. C., Ford, W. K., Jr., and Thonnard, N. 1976, *Ap. J.*, **208**, 662.
———. 1978, *Ap. J.*, **219**, 31.
Roberts, W. W. 1979, in *IAU Symposium No. 84, The Large Scale Characteristics of our Galaxy*, ed. W. B. Burton, in press.
Roberts, W. W., Huntley, J. M., and van Albada, G. D. 1979, *Ap. J.*, **233**, 67.
Rubin, V. C., Ford, W. K., Jr., and Kumar, C. K. 1973, *Ap. J.*, **181**, 61.
Rubin, V. C., Ford, W. K., Jr., and Peterson, C. J. 1975, *Ap. J.*, **199**, 39.
Rubin, V. C., Thonnard, N., and Ford, W. K., Jr. 1975, *Ap. J.*, **199**, 31.
Sandage, A. 1961, *The Hubble Atlas of Galaxies* (Washington: Carnegie Institution Pub., No. 618).

© American Astronomical Society • Provided by the NASA Astrophysics Data System

1980ApJ...238..808R

Sandage, A., and Brucato, R. 1979, *A.J.*, **84**, 472.
Sanders, R. H., and Tubbs, A. D. 1979, preprint.
Schechter, P. L., and Gunn, J. E. 1979, *Ap. J.*, **229**, 472.
Sersic, J. L., and Pastoriza, M. 1965, *Pub. A.S.P.*, **77**, 287.
Wolstoncroft, R. D., and Schempp, W. V. 1979, preprint.

VERA C. RUBIN: Department of Terrestrial Magnetism, Carnegie Institution of Washington, 5241 Broad Branch Road, N.W., Washington, DC 20015

© American Astronomical Society • Provided by the NASA Astrophysics Data System

1980ApJ...238..808R

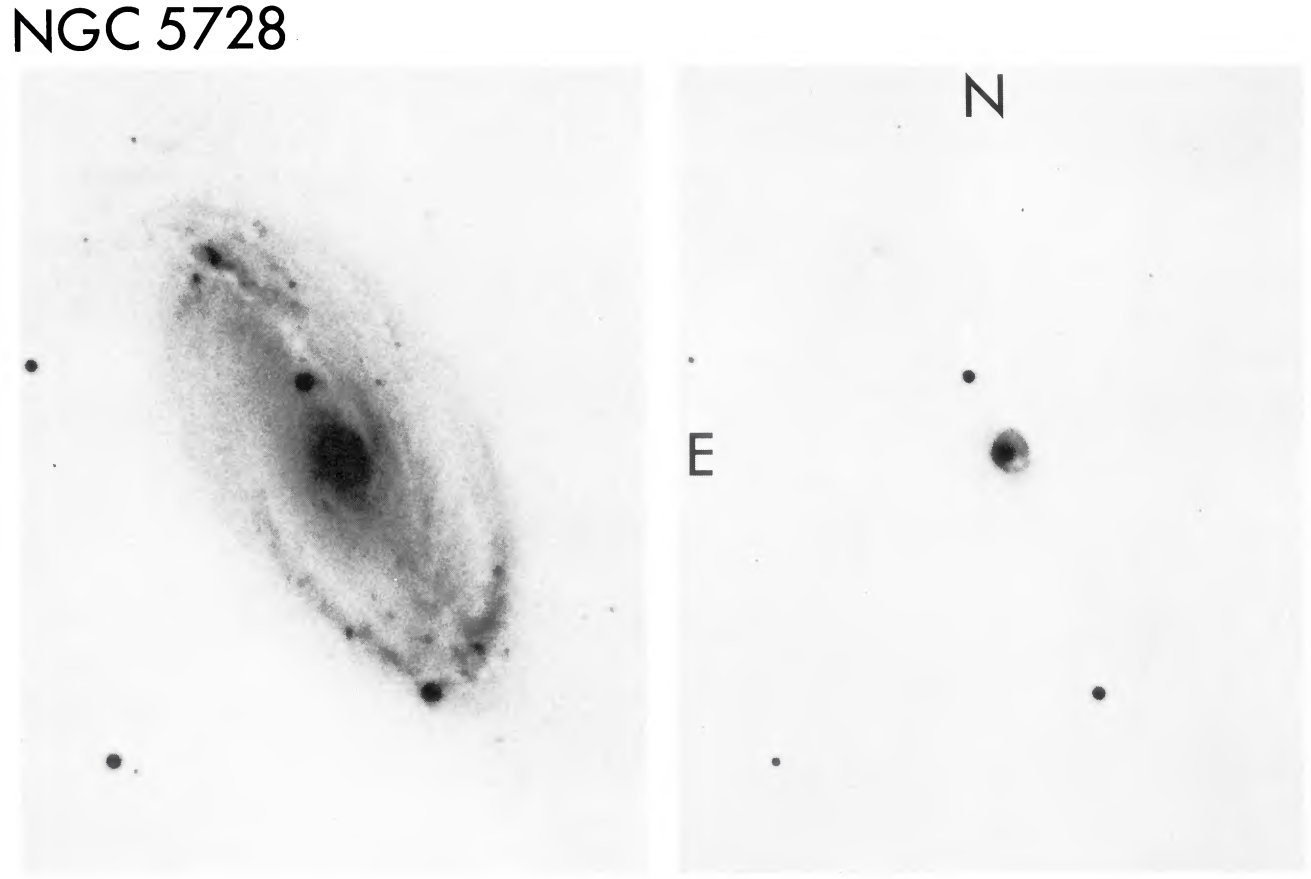

FIG. 1.—NGC 5228. (*Left*) Reproduction of the 2.5 m du Pont telescope plate, 103a-O + GG385, exposure 45 minutes, original scale 10.″8 mm^{-1}. (*Right*) 5 minute exposure showing nucleus tangent on E to nuclear ring. Star to SW of nucleus is 55″ distant; velocities have been determined to $r = 60''$.

RUBIN (*see* page 808)

© American Astronomical Society • Provided by the NASA Astrophysics Data System

1980ApJ...238..808R

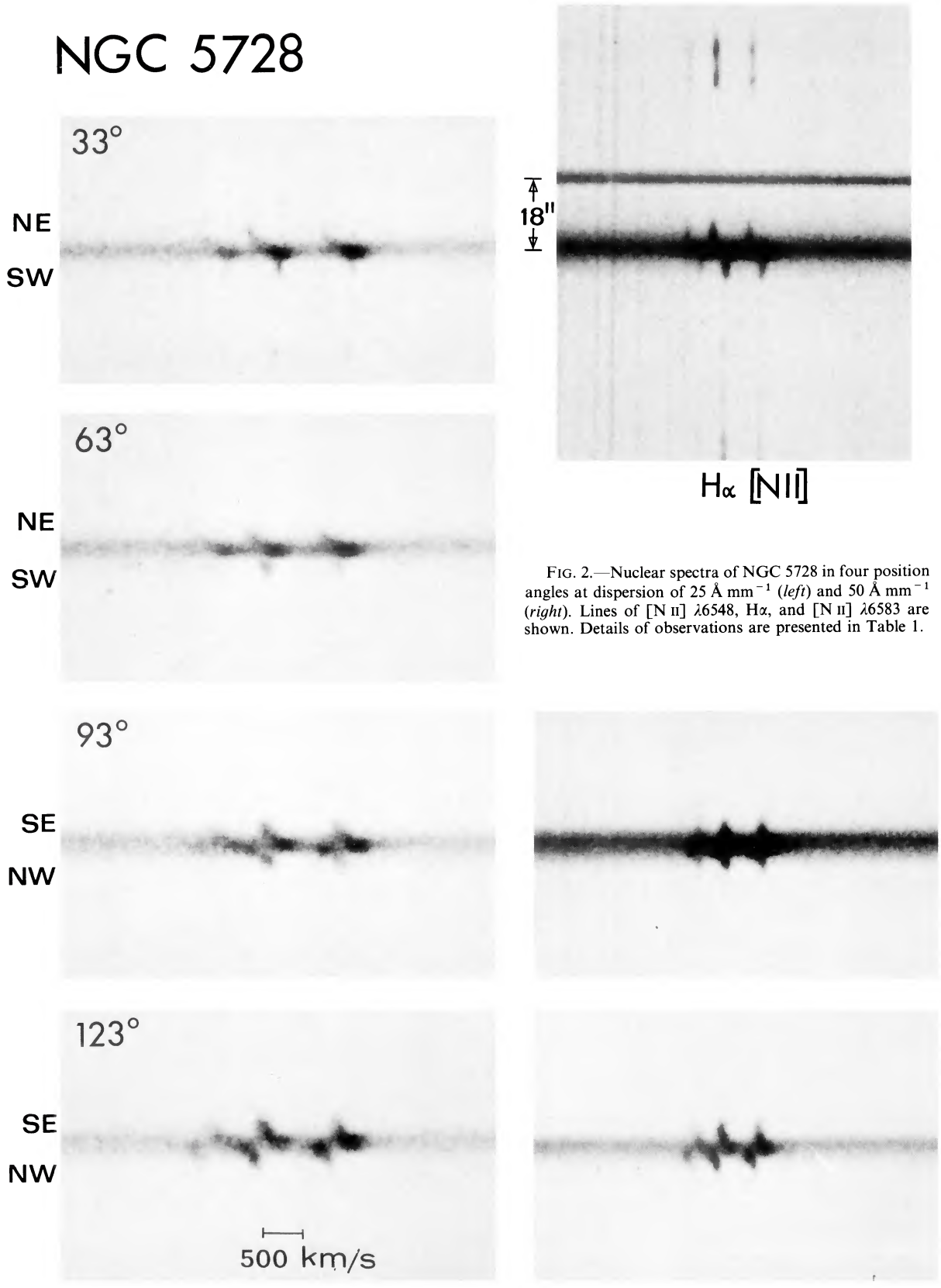

FIG. 2.—Nuclear spectra of NGC 5728 in four position angles at dispersion of 25 Å mm^{-1} (*left*) and 50 Å mm^{-1} (*right*). Lines of [N II] λ6548, Hα, and [N II] λ6583 are shown. Details of observations are presented in Table 1.

RUBIN (*see* page 808)

© American Astronomical Society • Provided by the NASA Astrophysics Data System